Nonlinear Dyn (2011) 66:731–743
DOI 10.1007/s11071-011-9946-0

ORIGINAL PAPER

A new semiactive nonlinear adaptive controller for structures using MR damper: Design and experimental validation

Saban Cetin · Erkan Zergeroglu · Selim Sivrioglu · Ismail Yuksek

Received: 16 June 2010 / Accepted: 6 January 2011 / Published online: 29 January 2011

Abstract In this study, we consider the vibration mitigation problem for a structural system using a magneto-rheological (MR) damper. For this purpose, through the use of Lyapunov-based design techniques, a nonlinear adaptive controller which can compensate the parametric uncertainties related to both the structural system and the MR damper has been constructed. To overcome effects of the unmeasurable internal dynamics of the MR damper on the controller, a filter-based design has been utilized. Experimental results performed on a six-degree-of-freedom (DOF) structure installed on a shaking table, illustrating the viability and the performance of the proposed method are also included.

Keywords Adaptive control · MR damper · Shaking table test · Structural control · Parameter estimation

S. Cetin (✉) · I. Yuksek
Faculty of Mechanical Engineering, Yildiz Technical University, Istanbul, Turkey
e-mail: scetin@yildiz.edu.tr

I. Yuksek
e-mail: yukseki@yildiz.edu.tr

E. Zergeroglu · S. Sivrioglu
Faculty of Engineering, Gebze Institute of Technology, Kocaeli, Turkey

E. Zergeroglu
e-mail: ezerger@bilmuh.gyte.edu.tr

S. Sivrioglu
e-mail: sselim@gyte.edu.tr

1 Introduction

Safety of structural systems against earthquake and wind loading is one of the most important matters in the life cycle of a building. Therefore, especially over the last three decades, the problem of vibration mitigation of structural system has been extensively targeted by control researchers from both theoretical and experimental points of view. Much work has been done in the area of structural control in terms of passive, semiactive, and active cases. As a result, many control algorithms and semiactive devices such as electro-rheological (ER) and magneto-rheological (MR) dampers have been investigated to earthquake hazard mitigation [7]. ER and MR dampers contain fluids that have capacity to change their viscosity, from a viscous fluid to a semisolid state, in milliseconds. Due to numerous advantages, mostly of practical usage, MR dampers are preferred to ER dampers [21]. MR dampers are semiactive devices that do not inject energy into system they are attached. They can absorb the vibratory energy that depends on the motion of the MR damper and input control voltage applied to them. Due to their mechanical simplicity, high dynamic range, low power requirements, low cost, large force capacity, and inherit stability, these devices are suitable for different applications such as suspension system and structural control [3, 20]. However, MR dampers exhibit nonlinear hysteresis behaviors when subjected to load. Therefore, one of the challenging issues for researchers working on systems equipped

with MR damper is choosing an accurate and suitable model to describe this nonlinear hysteresis behavior.

In order to describe the nonlinear hysteresis dynamic behavior of MR dampers, several models have been proposed, some of them have been investigated on quasistatic models [24, 27]. Although these models are useful for MR damper design, they are not sufficient to describe the MR damper nonlinear behavior under dynamic loading, specifically the nonlinear force velocity behavior [25, 29]. To overcome the forementioned problem, mainly two alternative models have been proposed in the literature; the first one is the Bouc–Wen hysteresis model proposed by Spencer et al. [21], Dyke et al. [3] implemented this proposed Bouc–Wen model of MR damper to a three-story steel frame building model. The second model proposed in [10, 11, 17, 22] is the LuGre hysteresis model extracted form the nonlinear friction model. Although Bouc–Wen model can accurately predict MR damper dynamics, it is too complex and difficult to use in parameter adaptation schemes such as adaptive controllers. Therefore in this work, the LuGre friction model was preferred over the Bouc–Wen model.

Nonlinearities and hysteresis dynamics in structures incorporating semiactive devices have considerable effects on the controller performance. On this account the other challenging issue for systems equipped with MR damper is the design of appropriate control laws. Various control algorithms used with the semiactive devices can be found in the literature. Leitmann [13] proposed a control strategy using Lyapunov's direct method for controlling ER dampers. This algorithm is based on reducing the response by minimizing the rate of change of the Lyapunov function. A similar approach investigated by McClamroch and Gavin [14], which is called decentralized bang-bang control. A Lyapunov function is used to represent the total vibratory energy in the system. Inaudi [8] proposed modulated a homogenous function algorithm for control of a variable friction damper. This algorithm is based on updating the normal force at the frictional interface. Clipped optimal control is proposed by Dyke et al. [3]. This algorithm is to design a linear optimal controller based on structural responses. These algorithms were also implemented to a six-degree-of-freedom structure with multiple MR dampers by Jansen and Dyke [9]. They concluded that the Lyapunov controller, clipped optimal controller, and modulated homogenous friction algorithm reduced the response of structure. Aldemir [1] proposed an optimal semiactive controller for a single-degree-of-freedom structure with a semiactive tune MR damper. This semiactive controller minimizes an integral norm of the main structure accelerations. The controller performance is compared with passive tuned mass case. The numerical simulations show that the performance of MR damper is always better than passive tuned case. Aldemir and Gavin [4, 5] are also utilized the optimal control to semiactive isolated structures. Ying et al. [30] proposed a stochastic optimal controller for ER and MR dampers. Sakai et al. [18] applied a bilinear H_∞ control and an adaptive inverse control for a semiactive isolated building. Villamizar et al. [23] investigated the performance of backstepping control for a structure equipped with multiple MR dampers. Cetin et al. [2] proposed an adaptive control scheme for a single-degree-of-freedom structure. Song et al. [20] proposed an adaptive semiactive control strategy for an MR suspension system. A modified sliding mode control technique for a structural system was designed by Neelakantan and Washington [15]. Yan and Zhou [26] proposed fuzzy logic and genetic algorithms for structures using MR damper. This abbreviated literature survey only accounts for a small subset of past research on the modeling and control of systems with MR damper. Nevertheless, results of all these studies show that the performance of the controlled system is highly dependent on the choice of control.

In this paper a novel nonlinear adaptive controller is proposed for vibration attenuation of structural systems equipped with MR damper. In the controller design, parametric uncertainties associated with both the structure and the semiactive actuator (MR damper) are considered. Nonlinear filters in conjunction with Lyapunov-based parameter estimators have been designed to compensate for the parametric uncertainties of the overall system. The proposed method is then experimentally validated on a six-floor structure. The rest of the paper is organized as follows. In Sect. 2, mathematical models of a six-DOF semiactive structural system and an MR damper are represented. Section 3 shows the general structure of control scheme and stability analysis. Experimental validation of control scheme is given in Sect. 4. Finally Sect. 5 provides concluding remarks.

2 Mathematical model and problem formulation

A schematic representation of the n-DOF building equipped with an MR damper considered in this work is given in Fig. 1. As most such structures, the MR damper is installed to the ground floor of the building via a rigid brace. The differential equation of motion governing the dynamical properties of the given semiactively controlled n-DOF structural system can be obtained to have the following form:

$$M_s\ddot{x} + C_s\dot{x} + K_s x = -Hf - M_s L\ddot{x}_g, \tag{1}$$

where $\ddot{x}(t)$, $\dot{x}(t)$, and $x(t) \in \Re^{n\times 1}$ are the floor acceleration, velocity, and displacement vectors, respectively, $M_s \in \Re^{n\times n}$ is the positive definite mass matrix, $C_s \in \Re^{n\times n}$ is the damping matrix, $K_s \in \Re^{n\times n}$ is the stiffness matrix, $f(t)$ is the control force input produced by the MR damper applied only to the ground floor via the location vector $H = [1\ 0\ \ldots\ 0]^T \in \Re^{n\times 1}$, and, finally, $\ddot{x}_g$ is the earthquake acceleration excitation with the vector $L = [1\ 1\ \ldots\ 1]^T \in \Re^{n\times 1}$ defining the influence of the earthquake excitation. Note that the dynamical model of (1) is formed by considering only the horizontal motion of the floors, the vertical and torsional motions are neglected for the ease of presentation. Also the displacement vector is explicitly defined as $x = [x_1\ x_2\ \ldots\ x_n]^T$ with x_i representing the ith floor motion.

The control force input to system of (1) is injected via an MR damper consisting of a hydraulic cylinder which houses a piston, a magnetic circuit, an accumulator, and MR fluid containing micron-sized magnetically polarizable ferrous particles (illustrated in Fig. 2). The damper piston contains damper coil and annular flow channels. The flow properties of MR fluids depend on magnetic field that is generated by input voltage in a magnetic coil installed at rod head. As discussed in the Introduction of the work, in order to describe the dynamic behaviors of MR dampers, several models have been proposed [10, 11, 17, 22]. In this work, similar to that of [22], the governing equation of the force produced is expressed using the LuGre-based model in the following form:

$$f = \sigma_a z + \sigma_0 z v + \sigma_1 \dot{z} + \sigma_2 \dot{x}_1 + \sigma_b \dot{x}_1 v, \tag{2}$$

$$\dot{z} = \dot{x}_1 - a_0|\dot{x}_1|z, \tag{3}$$

where σ_a, σ_b, and σ_i, $i = 0, 1, 2$, are scalar actuator parameters, $x_1(t)$ is the position of the ground floor

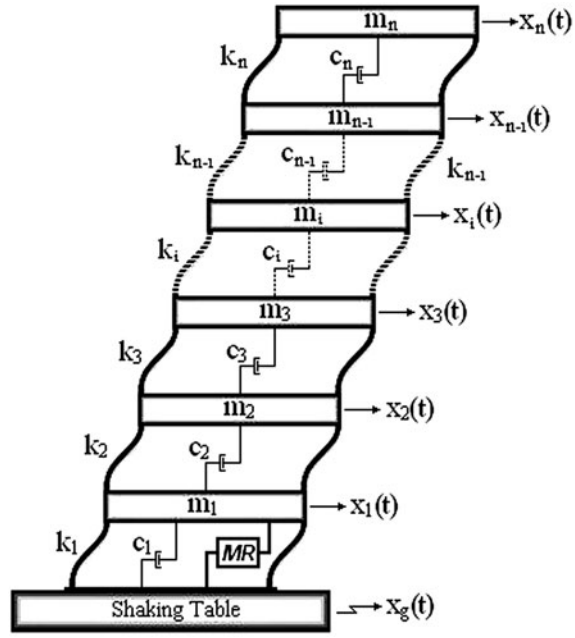

Fig. 1 The schematic representation of the structural system

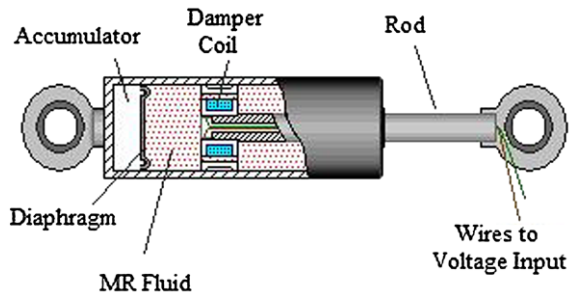

Fig. 2 Schematic of MR damper

where the damper is mounted, $z(t)$ is an internal state with the dynamics given in (3), and $v(t)$ is the controller input yet to be defined.

Unfortunately, due to the uncertain loading conditions, the system parameters of (1) are not precisely known; moreover, the model of (2)–(3) is merely a prediction of the semiactive damper, and extensive field tests are required to acquire the exact values of these parameters, which in practice is not always possible. Therefore the control problem presented here is to design the voltage input $v(t)$ of (2) which will ensure the absorbing of vibratory energy in a structure despite the inherent nonlinear characteristic of the actuator and parametric uncertainties of both the MR damper and structural system. To this end, combining (2) and (3),

we obtain the dynamics of the actuator as

$$f = \sigma_a z + \sigma_0 z v - \sigma_1 a_0 |\dot{x}_1| z + (\sigma_1 + \sigma_2)\dot{x}_1 + \sigma_b \dot{x}_1 v, \tag{4}$$

which can be written in the following compact form:

$$f = \rho_1 \theta_1 + \rho_2 \theta_2, \tag{5}$$

where the auxiliary vectors $\rho_1(z, v, \dot{x}_1)$ and $\rho_2(v, \dot{x}_1)$, and the uncertain parameter vectors θ_1 and θ_2 are explicitly defined as

$$\begin{aligned} \rho_1 &= \begin{bmatrix} z & zv & -|\dot{x}_1| z \end{bmatrix}, \qquad \rho_2 = \begin{bmatrix} \dot{x}_1 & \dot{x}_1 v \end{bmatrix}, \\ \theta_1 &= \begin{bmatrix} \sigma_a & \sigma_0 & \sigma_1 a_0 \end{bmatrix}^T, \qquad \theta_2 = \begin{bmatrix} \sigma_1 + \sigma_2 & \sigma_b \end{bmatrix}^T. \end{aligned} \tag{6}$$

Note that as the auxiliary signal ρ_1 of (5) contains the unmeasurable inner state z, an estimate of the input force from the MR damper would be in the form

$$\hat{f} = \hat{\rho}_1 \hat{\theta}_1 + \rho_2 \hat{\theta}_2, \tag{7}$$

which can be written as

$$\hat{f} = \hat{\theta}_{11} \hat{z} - \hat{\theta}_{13} |\dot{x}_1| \hat{z} + \hat{\theta}_{21} \dot{x}_1 + \left(\hat{\theta}_{12} \hat{z} + \hat{\theta}_{22} \dot{x}_1\right) v. \tag{8}$$

In (8), $\hat{z}$ is the estimate of the internal state variable, and $\hat{\theta}_{ij}$ represents a dynamic estimate of θ_{ij} of (6), yet to be constructed.

3 Semiactive adaptive control

3.1 Observer formulation

It is clear from (8) that, in order to formulate the estimated force, we need an observer for the internal state $z(t)$. Based on the subsequent stability analysis and assuming that the positive parameter a_0 defined in (3) can be obtained, we designed the following observer for $z(t)$:

$$\dot{\hat{z}} = \dot{x}_1 - a_0 |\dot{x}_1| \hat{z}. \tag{9}$$

The dynamics for the observation error defined as $\tilde{z} = z - \hat{z}$, can then be obtained using (3) and (9) as

$$\dot{\tilde{z}} = -a_0 |\dot{x}_1| \tilde{z}. \tag{10}$$

3.2 Controller formulation and design

Our main control objective is to regulate the displacement vector $x(t)$ of (1) for earthquake hazard mitigation of a structural system, and in order to provide a means to quantify the control objective, we define a filtered version of displacement vector $r(t) \in \Re^{n \times 1}$ as follows [19]:

$$r = \dot{x} + \alpha x, \tag{11}$$

where $\alpha \in \Re^{n \times n}$ is a constant, diagonal, and positive definite gain matrix. It is clear from the definition of (11) that, regulating $r(t)$ would enable us to regulate both $x(t)$ and $\dot{x}(t)$ at the same time. To obtain the dynamics of $r(t)$, we take the time derivative of (11) and premultiply the result by M_s of (1) to obtain

$$\begin{aligned} M_s \dot{r} &= M_s (\ddot{x} + \alpha \dot{x}) \\ &= Y \phi - H f, \end{aligned} \tag{12}$$

where (1) has been utilized, and

$$Y \phi = M_s \alpha \dot{x} - C_s \dot{x} - K_s x - M_s L \ddot{x}_g, \tag{13}$$

where $Y(\ddot{x}_g, \dot{x}, x) \in \Re^{n \times 3n}$ is the regression matrix of known and measurable signals, and $\phi \in \Re^{3n \times 1}$ is the vector containing the unknown system parameters. The regression matrix $Y(\ddot{x}_g, \dot{x}, x)$ can be explicitly defined to have the following form:

$$Y = \begin{bmatrix} Y_M & Y_C & Y_K \end{bmatrix} \tag{14}$$

with the auxiliary matrix variables Y_M, Y_C, and Y_K of proper dimensions defined as

$$\begin{aligned} Y_M &= \operatorname{diag}\left(\alpha_1 \dot{x}_1 - \ddot{x}_g \;\; \alpha_2 \dot{x}_2 - \ddot{x}_g \;\; \ldots \;\; \alpha_n \dot{x}_n - \ddot{x}_g\right), \\ Y_C &= \begin{bmatrix} -\dot{x}_1 & \dot{x}_2 - \dot{x}_1 & \ldots & 0 \\ 0 & \dot{x}_1 - \dot{x}_2 & \ldots & 0 \\ \vdots & \vdots & \ddots & \vdots \\ 0 & 0 & \ldots & -\dot{x}_n \end{bmatrix} \\ Y_K &= \begin{bmatrix} -x_1 & x_2 - x_1 & \ldots & 0 \\ 0 & x_1 - x_2 & \ldots & 0 \\ \vdots & \vdots & \ddots & \vdots \\ 0 & 0 & \ldots & -x_n \end{bmatrix}, \end{aligned} \tag{15}$$

where the notation $\operatorname{diag}(\cdot)$ is used to represent a square matrix having nonzero values only at its diagonal el-

ements with the given entries. Similarly, ϕ, the vector containing the uncertain but constant parameters can be partitioned as $\phi = [\phi_M\ \phi_C\ \phi_K]^T$ with

$$\begin{aligned}\phi_M &= \begin{bmatrix} m_1 & m_2 & \dots m_n \end{bmatrix},\\ \phi_C &= \begin{bmatrix} c_1 & c_2 & \dots & c_n \end{bmatrix},\\ \phi_K &= \begin{bmatrix} k_1 & k_2 & \dots & k_n \end{bmatrix}.\end{aligned} \tag{16}$$

Adding and subtracting the term $H\hat{f}$, to the right-hand side of (12), then utilizing (5) and (8), the open-loop dynamics for $r(t)$ can be obtained to have the following form:

$$\begin{aligned}M_s\dot{r} = {} & Y\phi + H\chi - Hu_x - H\rho_2\tilde{\theta}_2\\ & - H\big(\theta_{11}z - \hat{\theta}_{11}\hat{z} + \theta_{12}vz\\ & - \hat{\theta}_{12}v\hat{z} - \theta_{13}|\dot{x}_1|z + \hat{\theta}_{13}|\dot{x}_1|\hat{z}\big),\end{aligned} \tag{17}$$

where the auxiliary variables χ and u_x are explicitly defined as

$$\begin{aligned}\chi &= \big(-\hat{\theta}_{11}\hat{z} + \hat{\theta}_{13}|\dot{x}_1|\hat{z} - \hat{\theta}_{21}\dot{x}_1\big),\\ u_x &= \big(\hat{\theta}_{12}\hat{z} + \hat{\theta}_{22}\dot{x}_1\big)v.\end{aligned} \tag{18}$$

Based on the subsequent stability analysis and controller formulation, we require the signal Hu_x to have the form

$$\begin{aligned}Hu_x = {} & Kr + H\chi + Y\hat{\phi}\\ & + H\big(-\hat{\theta}_{11}\zeta_1 - \hat{\theta}_{12}\zeta_2 v + \hat{\theta}_{13}|\dot{x}_1|\zeta_3\big).\end{aligned} \tag{19}$$

Utilizing this, the control input voltage to MR damper is derived as

$$Hv = \frac{Kr + H\chi + Y\hat{\phi} + H(-\hat{\theta}_{11}\zeta_1 + \hat{\theta}_{13}|\dot{x}_1|\zeta_3)}{\hat{\theta}_{12}\hat{z} + \hat{\theta}_{22}\dot{x}_1 + \hat{\theta}_{12}\zeta_2}, \tag{20}$$

where K is a constant positive definite diagonal control gain matrix, $\hat{\phi}(t)$, $\hat{\theta}_{21}(t)$, $\hat{\theta}_{22}(t)$, $\hat{\theta}_{11}(t)$, $\hat{\theta}_{12}(t)$, and $\hat{\theta}_{13}(t)$ are the dynamic estimates of the unknown but constant system and MR damper parameters updated according to

$$\begin{aligned}\dot{\hat{\phi}} &= \Gamma_\phi Y^T r,\\ \dot{\hat{\theta}}_2 &= -\Gamma_2\rho_2^T H^T r,\\ \dot{\hat{\theta}}_{11} &= -\gamma_1(\hat{z} + \zeta_1)H^T r,\\ \dot{\hat{\theta}}_{12} &= -\gamma_2 v(\hat{z} + \zeta_2)H^T r,\\ \dot{\hat{\theta}}_{13} &= \gamma_3|\dot{x}_1|(\hat{z} + \zeta_3)H^T r,\end{aligned} \tag{21}$$

where Γ_ϕ, Γ_2 are positive definite, diagonal, adaptation gain matrices with proper dimensions, and γ_i with $i = 1, 2, 3$ are positive scalar adaptation gains. Also ζ_1, ζ_2, and ζ_3 are auxiliary filters designed to be updated according to the following formulations:

$$\begin{aligned}\dot{\zeta}_1 &= -a_0|\dot{x}_1|\zeta_1 - H^T r,\\ \dot{\zeta}_2 &= -a_0|\dot{x}_1|\zeta_2 - vH^T r,\\ \dot{\zeta}_3 &= -a_0|\dot{x}_1|\zeta_3 + |\dot{x}_1|H^T r.\end{aligned} \tag{22}$$

Notice that in order to ensure the boundedness of the control signal of (19), its denominator has to be artificially kept away from zero via a projection algorithm. A block diagram representation of the controller proposed in this work is presented in Fig. 3. Substituting (19) back into (17), the closed-loop dynamics for $r(t)$ is obtained as follows:

$$\begin{aligned}M_s\dot{r} = {} & -Kr + Y\tilde{\phi} - H\rho_2\tilde{\theta}_2\\ & - H\big(\theta_{11}z - \hat{\theta}_{11}(\hat{z} + \zeta_1)\big)\\ & - H\big(\theta_{12}vz - \hat{\theta}_{12}v(\hat{z} + \zeta_2)\big)\\ & + H\big(\theta_{13}|\dot{x}_1|z - \hat{\theta}_{13}|\dot{x}_1|(\hat{z} + \zeta_3)\big),\end{aligned} \tag{23}$$

where $\tilde{\phi}$ and $\tilde{\theta}_{ij}$ are the used to represent the difference between the actual and estimates parameters as follows:

$$\begin{aligned}\tilde{\phi} &= \phi - \hat{\phi},\\ \tilde{\theta}_{ij} &= \theta_{ij} - \hat{\theta}_{ij}.\end{aligned} \tag{24}$$

Adding and subtracting the terms of $H(\theta_{11}(\hat{z} + \zeta_1))$, $H(\theta_{12}v(\hat{z} + \zeta_2))$, and $H(\theta_{13}|\dot{x}_1|(\hat{z} + \zeta_3))$ to (23) and rearranging the terms, the closed-loop error dynamics can be written in the following advantageous form:

$$\begin{aligned}M_s\dot{r} = {} & -Kr + Y\tilde{\phi} - H\rho_2\tilde{\theta}_2\\ & + H\big(-\tilde{\theta}_{11}(\hat{z} + \zeta_1) - \theta_{11}(\tilde{z} - \zeta_1)\big)\\ & + H\big(-\tilde{\theta}_{12}v(\hat{z} + \zeta_2) - \theta_{12}v(\tilde{z} - \zeta_2)\big)\\ & + H\big(\tilde{\theta}_{13}|\dot{x}_1|(\hat{z} + \zeta_3) + \theta_{13}|\dot{x}_1|(\tilde{z} - \zeta_3)\big).\end{aligned} \tag{25}$$

At this stage we are ready to propose the following theorem.

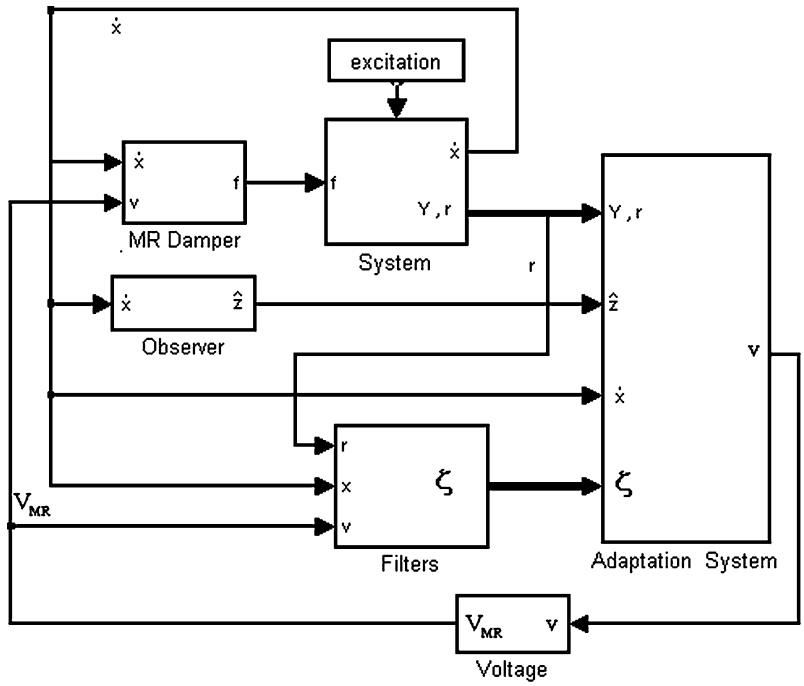

Fig. 3 Block diagram of overall control scheme

3.3 Stability analysis

Theorem 1 *For the semiactively controlled n-DOF structural system given in* (1)*, the observer–controller couple described by* (20) *and* (9) *with the adaptation laws of* (21) *and the filters given in* (22) *guarantees asymptotic regulation of the structural system in the sense that*

$$\lim_{t\to\infty}(x,\dot{x})=0, \tag{26}$$

provided that

$$\beta=\hat{\theta}_{12}\hat{z}+\hat{\theta}_{22}\dot{x}_1+\hat{\theta}_{12}\zeta_2 \tag{27}$$

is kept artificially away from zero.

Proof We begin our proof by defining the following nonnegative function:

$$\begin{aligned}V=&\frac{1}{2}r^T M_s r+\frac{1}{2}\tilde{z}^2+\frac{1}{2}\tilde{\phi}^T\Gamma_\phi^{-1}\tilde{\phi}\\&+\frac{1}{2}\tilde{\theta}_2^T\Gamma_2^{-1}\tilde{\theta}_2+\frac{1}{2}\frac{1}{\gamma_1}\tilde{\theta}_{11}^2+\frac{1}{2}\frac{1}{\gamma_2}\tilde{\theta}_{12}^2\\&+\frac{1}{2}\frac{1}{\gamma_3}\tilde{\theta}_{13}^2+\frac{1}{2}\theta_{11}(\tilde{z}-\zeta_1)^2\\&+\frac{1}{2}\theta_{12}(\tilde{z}-\zeta_2)^2+\frac{1}{2}\theta_{13}(\tilde{z}-\zeta_3)^2.\end{aligned} \tag{28}$$

Taking the time derivative of (28), substituting for (25), (9), (20), (21), and (22), and cancelling common terms, we obtain

$$\begin{aligned}\dot{V}=&-r^T Kr-a_0|\dot{x}_1|\tilde{z}^2\\&-\theta_{11}a_0|\dot{x}_1|(\tilde{z}-\zeta_1)^2\\&-\theta_{12}a_0|\dot{x}_1|(\tilde{z}-\zeta_2)^2\\&-\theta_{13}a_0|\dot{x}_1|(\tilde{z}-\zeta_3)^2,\end{aligned} \tag{29}$$

where the last four terms are always negative, enabling us to upper bound (29) as

$$\dot{V}\le -r^T Kr. \tag{30}$$

Due to the structure of (28) and (30), $V\in\mathcal{L}_\infty$ (is bounded); therefore, $r(t)$, $\tilde{z}$, $\tilde{\phi}$, and $\tilde{\theta}\in\mathcal{L}_\infty$. Furthermore, from (30) it is straightforward to show that $r(t)\in\mathcal{L}_2$ (square-integrable). Using standard signal chasing arguments, we can show that all of the signals in the closed-loop system are bounded. We now use closed-loop error system and the boundedness of all signals to prove that $\dot{r}(t)$ and $\dot{\tilde{z}}$ are also bounded (from (25) and (9), respectively). We can now apply Barbalat's lemma [12] to conclude the result given in (26). □

Table 1 Identified values of structure

M	kg	C	N · s/m	K	N/m
m_1	108	c_1	25	k_1	109150
m_2	113	c_2	26	k_2	138150
m_3	106	c_3	27	k_3	144090
m_4	106	c_4	26	k_4	151430
m_5	98	c_5	27	k_5	145890
m_6	113	c_6	31	k_6	148570

3.4 Semiactive controller implementation

The input voltage given in (20) can be implemented to structure as follows:

$$V_{\mathrm{MR}} = \begin{cases} 0 & \text{if } v \le 0, \\ v & \text{if } 0 < v \le V_{\max}, \\ V_{\max} & \text{otherwise}, \end{cases} \tag{31}$$

where $V_{\max} = 4$ V is the maximum voltage applied to MR damper. β is adjusted according to

$$\beta = \begin{cases} \epsilon & \text{if } -\epsilon \le \beta \le \epsilon, \\ \beta & \text{otherwise.} \end{cases} \tag{32}$$

4 Experimental validation

In order to illustrate the effectiveness of the proposed nonlinear adaptive controller, we constructed an experimental setup at Machine Theory System Dynamics and Control Laboratory, Yildiz Technical University. A photograph of experimental setup is shown in Fig. 4, and a schematic representation of the setup is depicted in Fig. 5. As shown in the figures, the model used in our experimentations is a single-bay six-story frame building with steel floors weighing approximately 107 kg. The floors are bolted in eight columns which are made of spring steel beams. These beams are 50-mm wide and 3-mm thick. The interstory height is 250 mm. In order to obtain an approximation of the structural parameters, a system identification method based on Hilbert transform [28] has been applied. The parameters obtained are presented in Table 1. Note that $C_s = \alpha M_s + \beta K_s$, where $\alpha = 0.0265$ and $\beta = 0.0001143$.

To obtain estimates of the MR damper parameters, we conducted preliminary experiments where the

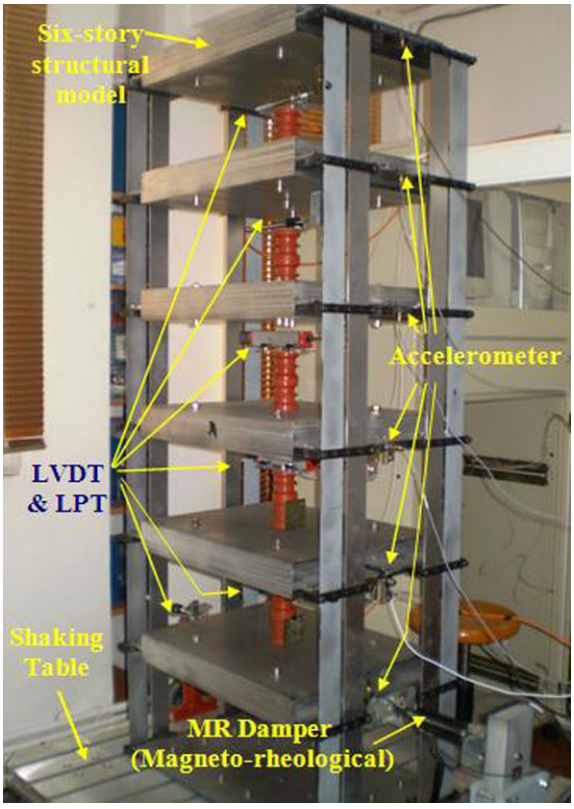

Fig. 4 A photograph of experimental structure

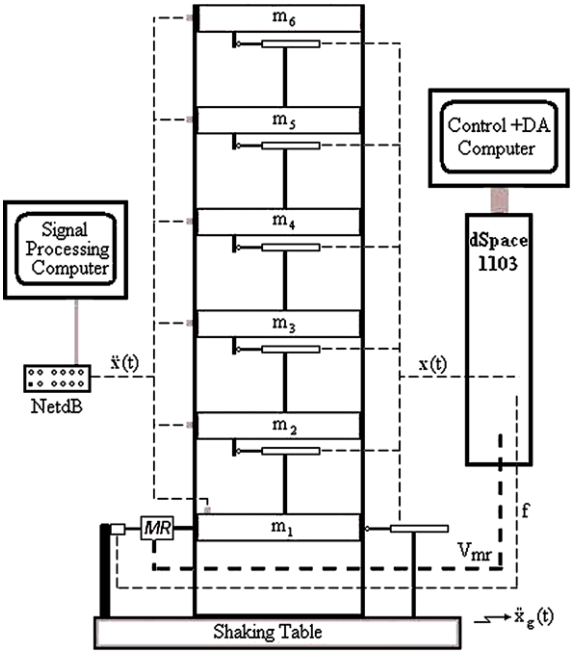

Fig. 5 Schematic of experimental setup

force produced by MR damper is measured when random displacement inputs are applied. During these initial trails, MR damper voltage is set to 2 V. Velocity input of the experiments is given in Fig. 6, and the corresponding parameter estimates of MR damper are given in Table 2. The estimated force and measured force of MR damper are given in Fig. 7. In addition, force-velocity and force-displacement results of MR damper are shown in Fig. 8.

An electromechanically driven shake table is used to introduce one-dimensional ground acceleration. dSpace ACE Kit 1103 hardware and software packages are used for data acquisition and control imple-

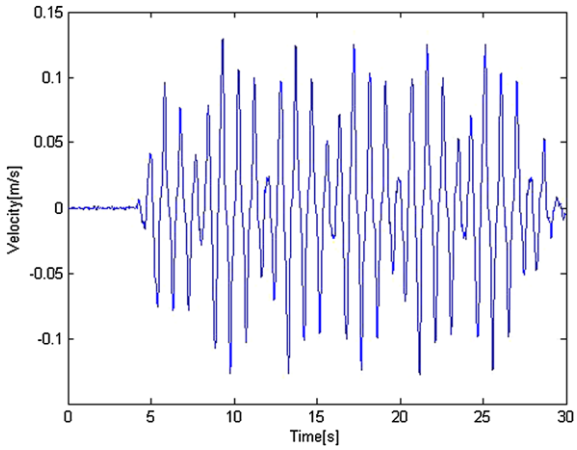

Fig. 6 Velocity input

Table 2 Experimentally obtained values for the MR damper parameters

$\hat{\theta}_{11}$	$\hat{\theta}_{12}$	$\hat{\theta}_{13}$	$\hat{\theta}_{21}$	$\hat{\theta}_{22}$
76000	320000	4500	1156.5	315

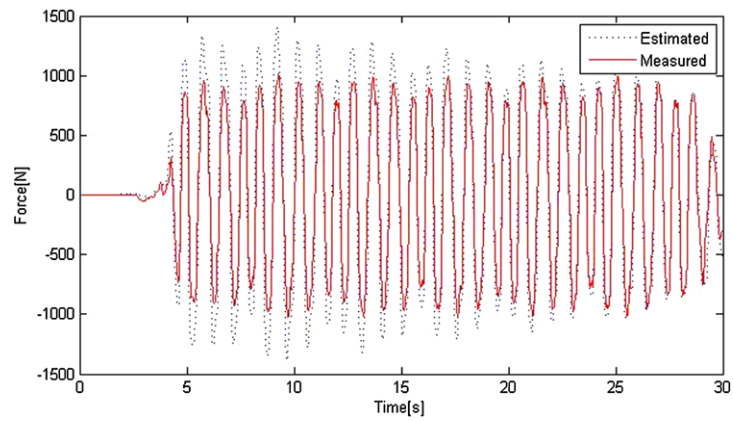

Fig. 7 Measured and estimated force of MR damper

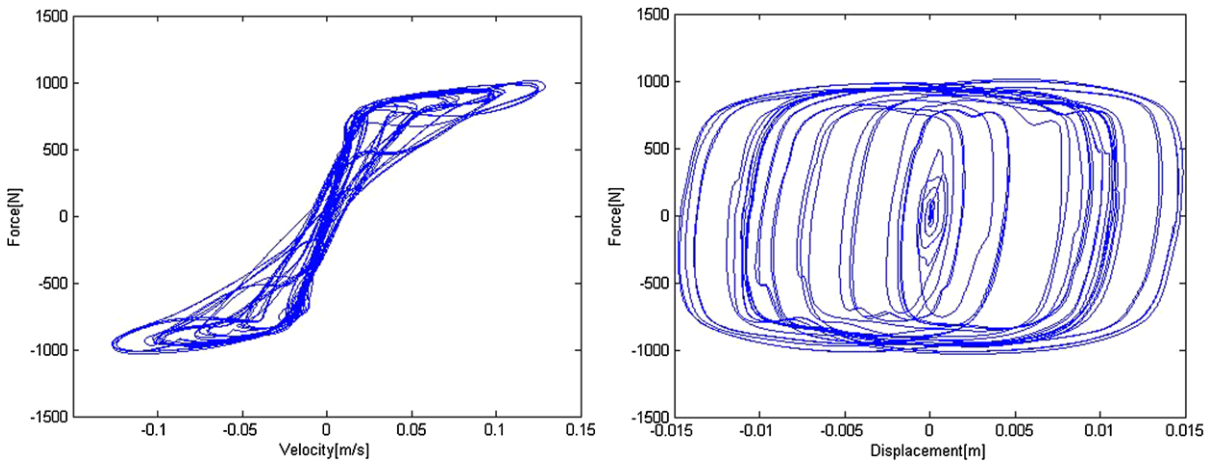

Fig. 8 Characteristics of MR damper

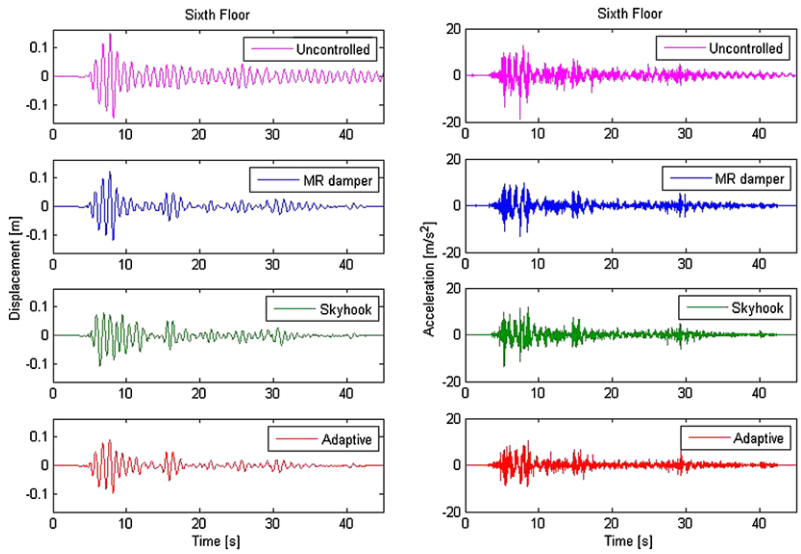

Fig. 9 Sixth floor displacement and acceleration

mentation. For displacement measurements, variety of sensors including three Waycon linear variable displacement transformers (LVDT) and three Opkon linear position transducers (LPT) are placed to different floors of the structure. To measure the force applied the MR damper during the experiments, a BKjaer force transducer has been used, and Endevco Model 133 signal conditioner is placed between the force transducer and dSpace Kit. Acceleration measurements are obtained using four BKjaer accelerometers and two Dytran accelerometers, and an 8-channel NetdB real-time analyzer is used for signal processing of acceleration data.

Four sets of experiments are performed: first, an uncontrolled (without MR damper), secondly, passive damper where MR damper is connected to the system but is left passive (zero volts applied to its terminals), thirdly, a skyhook controller [6] is implemented to the system, and lastly the damper is attached and excited with the proposed adaptive controller. For all experiments, a scaled (70%) NS component of the 1940 El Centro seismic data is used as ground acceleration. The results are compared among the cases uncontrolled, the MR damper (passive off), skyhook control, and proposed adaptive control. For the proposed adaptive controller, the controller gains were selected as

$$K = \mathrm{diag}\{10^5 \;\; 1 \;\; 1 \;\; 1 \;\; 1 \;\; 1\},$$
$$\alpha = \mathrm{diag}\{1 \;\; 100 \;\; 100 \;\; 100 \;\; 100 \;\; 100\}, \tag{33}$$

with the adaptation gains set to

$$\begin{aligned}\Gamma_\phi = \mathrm{diag}\{&1.5\times10^4 \;\; 1.5 \;\; 0.7 \;\; 0.475 \;\; 0.365 \;\; 0.3785\\ &594 \;\; 75 \;\; 150 \;\; 232 \;\; 468 \;\; 7 \;\; 3.65\times10^7\\ &1.65\times10^5 \;\; 3.876\times10^5 \;\; 5.55\times10^5\\ &2\times10^5 \;\; 0.16575\times10^5\},\end{aligned} \tag{34}$$

$$\Gamma_2 = \mathrm{diag}\{26500 \;\; 18000\},$$
$$\gamma_1 = 2.35\times10^7, \qquad \gamma_2 = 6.65\times10^7, \quad \text{and}$$
$$\gamma_3 = 3.5\times10^7.$$

Figure 9 shows the time histories of the sixth floor's displacement and acceleration. The corresponding frequency responses of sixth floor are illustrated in Fig. 10. The dotted line denotes the uncontrolled case, the dashed line expresses the passive off case, the dashdot line depicts the skyhook controller, and the solid line represents the proposed controller. From the time histories of top floor, it can be seen that the displacement peaks around 0.15 m and the acceleration peaks at 20 m/s^2 in uncontrolled case. The MR damper reduces the vibration levels of structural system in both passive off case and controlled cases. Specifically, adaptive controller provided a large amount of decrease in the acceleration responses of the structure.

The parameter estimates of both the structural system and the MR damper are presented in Figs. 12–15. Specifically, Fig. 12 illustrates ϕ_i $(i = 1, 2, \ldots, 6)$

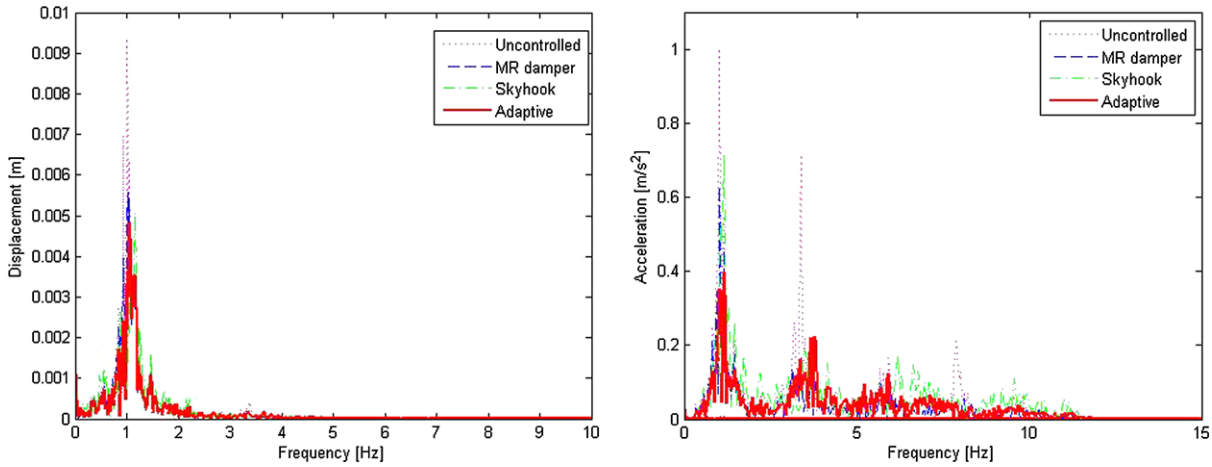

Fig. 10 Frequency response sixth floor displacement and acceleration

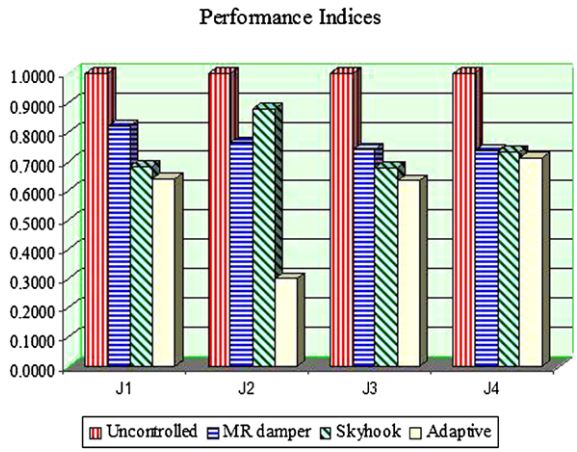

Fig. 11 Comparison of performance indices

corresponding to the estimates of the mass-related parameters of the structure, Fig. 13 illustrates ϕ_i $(i = 7, 8, \ldots, 12)$ that are the estimates of the damping coefficient-related parameters of the structure, Fig. 14 illustrates ϕ_i $(i = 13, 14, \ldots, 18)$ the estimates of the stiffness coefficients-related parameters of the structure. Figure 15 shows the estimates of the MR damper parameters. During the experimental studies, the initial values of the structural system parameter estimated were set to

$$\begin{aligned} &\hat{\phi}_i(0) = 0, \quad i = 1, 2, \ldots, 6, \\ &\hat{\phi}_j(0) = 50, \quad j = 7, 8, \ldots, 12, \\ &\hat{\phi}_k(0) = 175000, \quad k = 13, 14, \ldots, 18, \end{aligned} \tag{35}$$

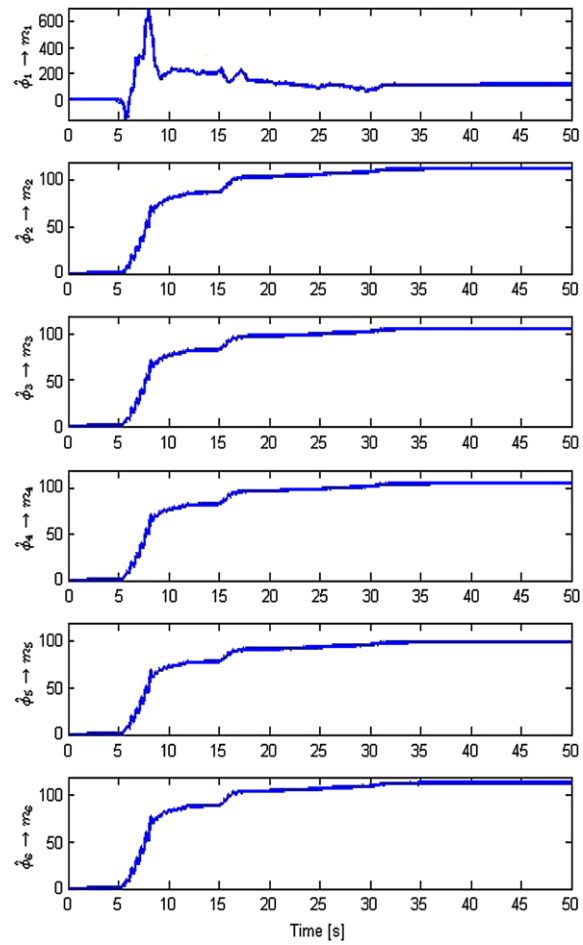

Fig. 12 Estimates of mass parameters

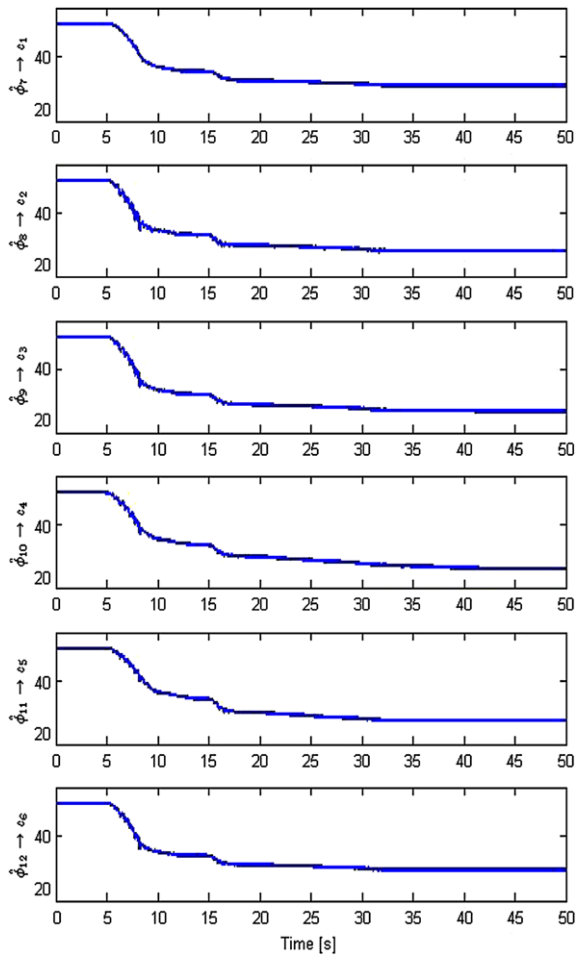

Fig. 13 Estimates of damping coefficients

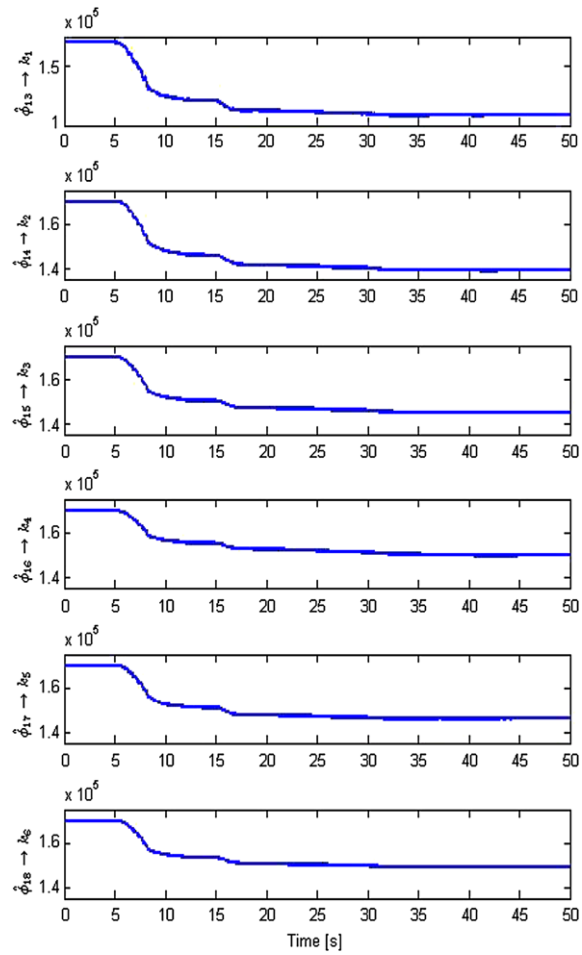

Fig. 14 Estimates of stiffness parameters

and the initial values of the MR damper parameter estimates were selected as

$$\hat{\theta}_1(0) = \left[10^5 \;\; 4\times 10^5 \;\; 3.5\times 10^5\right]^T,$$
$$\hat{\theta}_2(0) = \left[2\times 10^3 \;\; 10^3\right]^T. \tag{36}$$

The experimental results were then evaluated with four different performance indices defined by Ohtori et al. [16] to validate the effectiveness of the proposed method. The first two criteria are related with peak levels of vibration and are defined as follows:

$$J_1 = \max\left\{\frac{\max_{t,i}|d_i(t)|}{\delta^{\max}}\right\},$$
$$J_2 = \max\left\{\frac{\max_{t,i}|\ddot{x}_i(t)|}{|\ddot{x}_i^{\max}(t)|}\right\} \tag{37}$$

over the interval $i = 1, 2, \ldots, 6$, where J_1 is the interstory drift ratio, and J_2 means the level acceleration. $d_i(t)$ and $\ddot{x}_i(t)$ define the interstory drift and acceleration of the ith story. $\delta^{\max}$ and $\ddot{x}_i^{\max}(t)$ are the maximum interstory drift and acceleration of the uncontrolled structure, respectively. Note that the heights of all stories are equal, enabling us to neglected the term in the first and third criteria apart from the original forms. Other two criteria are defined by the norm forms of J_1 and J_2 as

$$J_3 = \max\left\{\frac{\max_{t,i}\|d_i(t)\|}{\|\delta^{\max}\|}\right\},$$
$$J_4 = \max\left\{\frac{\max_{t,i}\|\ddot{x}_i(t)\|}{\|\ddot{x}_i^{\max}(t)\|}\right\}. \tag{38}$$

Comparison of the performance indices are illustrated in Fig. 11. As can be viewed, the proposed controller

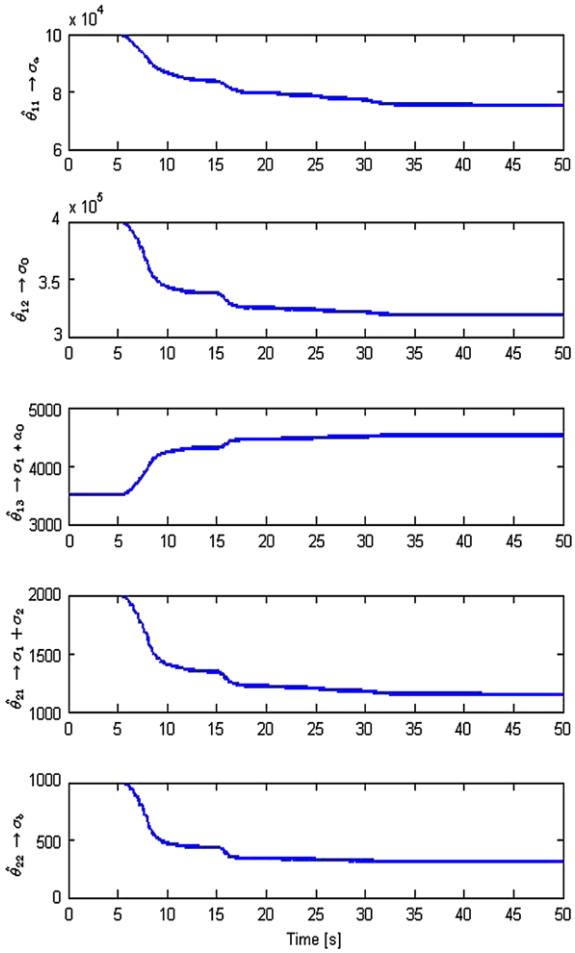

Fig. 15 Estimates of MR damper parameters

reduces both displacement and acceleration responses of the structural system and has the best results in all performance indices. Specifically, adaptive controller has a great decrease in peak response value of acceleration. Comparing the passive, skyhook, and controlled cases in all situations, it can be concluded that the proposed controller is quite effective and suppresses the vibration of the structural system.

Experimental studies clearly validated that the proposed nonlinear semiactive adaptive controller scheme reduces not only the displacement but also the acceleration responses of the structure.

5 Conclusions

In this study, the design of a nonlinear adaptive controller scheme for the vibration mitigation of a structural system using a semiactive actuator (an MR damper) has been presented. The proposed nonlinear controller guarantees asymptotic regulation of the structural system despite the parametric uncertainties in the dynamics of the system and the semiactive actuator. Extensive experimental studies were performed to validate the effectiveness and the implementability of proposed nonlinear semiactive adaptive controller scheme.

References

1. Aldemir, U.: Optimal control of structures with semiactive-tune mass dampers. J. Sound Vib. **266**(4), 847–874 (2003)
2. Cetin, S., Sivrioglu, S., Zergeroglu, E., Yuksek, I.: Adaptive control of structures with MR damper. In: 3rd IEEE Multi-Conference on Systems and Control, St. Petersburg, Russia, 8–10 July (2009)
3. Dyke, S.J., Spencer, B.F. Jr., Sain, M.K., Carlson, J.D.: Modeling and control of magnetorheological dampers for seismic response reduction. Smart Mater. Struct. **5**, 565–575 (1996)
4. Gavin, H.P., Aldemir, U.: Optimal control of earthquake response semiactive isolation. J. Eng. Mech. **131**(8), 769–776 (2005)
5. Gavin, H.P., Aldemir, U.: Optimal semiactive control of structures with isolated base. Int. Appl. Mech. **132**(7), 705–713 (2006)
6. Hiemenz, G.J., Choi, Y.T., Wereley, N.M.: Seismic control of civil structures utilizing semi-active MR braces. Comput.-Aided Civ. Infrastruct. Eng. **18**, 31–44 (2003)
7. Housner, G.W., et al.: Structural control: past, present, and future. J. Eng. Mech. ASCE **123**(9), 897–971 (1997)
8. Inaudi, J.A.: Modulated homogeneous friction: A semi-active damping strategy. Earthq. Eng. Struct. Dyn. **26**(3), 361–376 (1997)
9. Jansen, M.L., Dyke, S.J.: Semiactive control strategies for MR dampers: Comparative study. J. Eng. Mech. ASCE **126**(8), 795–803 (2000)
10. Jimenez, R., Alvarez, L.: Real time identification of structures with magnetorheological dampers. In: Proceedings of the 41st IEEE Conference on Decision and Control, pp. 1017–1022 (2002)
11. Jimenez, R., Alvarez-Icaza, L.: LuGre friction model for a magnetorheological damper. Struct. Control Heal. Monit. **12**, 91–116 (2005)
12. Krstic, M., Kanellakopoulos, I., Kokotovic, P.: Nonlinear and Adaptive Control Design. Wiley, New York (1995)
13. Leitmann, G.: Semiactive control for vibration attenuation. J. Intell. Mater. Syst. Struct. **5**, 841–846 (1994)
14. McClamroch, N.H., Gavin, H.P.: Closed loop structural control using electrorheological dampers. In: Proc. of the Amer. Ctrl. Conf., Seattle, Washington, pp. 4173–4177 (1995)
15. Neelakantan, V.J., Washington, G.N.: Vibration control of structural systems using MR dampers and a 'modified' sliding mode control technique. J. Intell. Mater. Syst. Struct. **19**(2), 211–224 (2008)

16. Ohtori, Y., Christenson, R.E., Spencer, B.F., Dyke, S.J.: Benchmark control problem for seismically excited nonlinear buildings. J. Eng. Mech. ASCE **130**, 366–385 (2004)
17. Sakai, C., Ohmori, H., Sano, A.: Modeling of MR damper with hysteresis for adaptive vibration control. In: Proceedings of the 42nd IEEE Conference on Decision and Control, Maui, Hawaii, USA, December (2003)
18. Sakai, C., Terasawa, T., Sano, A.: Integration of bilinear H_∞ control and adaptive inverse control for semi-active vibration isolation of structures. In: Proceedings of the 44th IEEE Conference on Decision and the European Control Conference 2005, Seville, Spain, 12–15 December (2005)
19. Slotine, J.J., Li, W.: Applied Nonlinear Control. Prentice Hall, Englewood Cliff (1991)
20. Song, X., Ahmadian, M., Southward, S., Miller, L.R.: An adaptive semiactive control algorithm for magnetorheological suspension systems. J. Vib. Acoust. **127**, 493–502 (2005)
21. Spencer, B.F. Jr., Dyke, S.J., Sain, M.K., Carlson, J.D.: Phenomenological model of a Magnetorheological Damper. J. Eng. Mech. ASCE **123**(3), 230–238 (1997)
22. Terasawa, T., Sakai, C., Ohmori, H., Sano, A.: Adaptive identification of MR damper for vibration control. In: 43rd IEEE Conference on Decision and Control, Atlantis, Paradise Island, Bahamas, 14–17 December (2004)
23. Villamizar, R., Ningsu, L., Dyke, S.J., Vehi, J.: Experimental verification of backstepping controllers for magnetorheological MR dampers in structural control. In: Proceedings of 13th Mediterranean Conference on Control and Automation, Limassol, Cyprus, 27–29 June (2005)
24. Wereley, N.M., Pang, L.: Nondimensional analysis of semiactive electrorheological and magnetorheological dampers using approximate parallel plate models. Smart Mater. Struct. **7**, 732–743 (1998)
25. Wereley, N.M., Pang, L., Kamath, G.M.: Idealized hysteresis modeling of electrorheological and magnetorheological dampers. J. Intell. Mater. Syst. Struct. **9**(8), 642–649 (1998)
26. Yan, G., Zhou, L.L.: Integrated fuzzy logic and genetic algorithms for multi-objective control of structures using MR dampers. J. Sound Vib. **296**, 368–382 (2006)
27. Yang, G., Spencer, B.F. Jr., Carlson, J.D., Sain, M.K.: Large-scale MR fluid dampers: Modeling and dynamic performance considerations. Eng. Struct. **24**, 309–323 (2002)
28. Yang, J.N., Lei, Y., Pan, S., Huang, N.: System identification of linear structures based on Hilbert–Huang spectral analysis. Part I: Normal modes. Earthquake Eng. Struct. Dyn. **32**, 1443–1467 (2003)
29. Yang, G., Spencer, B.F., Jung, H.-J., Carlson, J.D.: Dynamic modeling of large-scale magnetorheological damper systems for civil engineering applications. J. Eng. Mech. (ASCE) **130**(9), 1107–1114 (2004)
30. Ying, Z.G., Zhu, W.Q., Soong, T.T.: A stochastic optimal semi-active control strategy for ER/MR dampers. J. Sound Vib. **259**(1), 45–62 (2003)